Enthalpic Stabilization of Brush-Coated Particles in a Polymer Melt

Itamar Borukhov*,† and Ludwik Leibler‡

Unité Mixte de Recherche CNRS/Elf-Atochem (UMR 167), 95 rue Danton, B.P. 108, 92303 Levallois-Perret Cedex, France

Received July 30, 2001; Revised Manuscript Received March 18, 2002

ABSTRACT: The interaction between spherical particles covered with end-grafted polymers (brushes) immersed in a polymer melt is studied theoretically. It has been known for some time that two densely grafted brushes may attract each other in the presence of a chemically identical polymer melt. In this study we show that this attraction can be eliminated by choosing the melt material to be such that the Flory interaction parameter of the melt chains with the grafted ones is negative ($\chi < 0$). This effect is accompanied by a change in the structure of the brush from a dry brush, where the melt chains do not penetrate deeply into the brush, to a wet brush, where the melt chains penetrate the brush and force the grafted chains to extend into the melt. Scaling arguments are used to describe how the structure of a single brush depends on the Flory interaction parameter, the grafting density, and the indices of polymerization of the grafted and free chains. The density profiles and the interactions between the particles are calculated by solving numerically the self-consistent field equations of the system within the Derjaguin approximation. The effect of van der Waals interactions between brushes is studied by taking into account the particle−brush contrast as well as that of the brush−melt interfaces.

I. Introduction

A polymer brush consists of long polymer chains terminally attached (grafted) to a surface at one end.[1−6] Brushes play an important role in colloidal science as a way to protect colloidal suspensions from flocculation. The grafted layer surrounding the colloids inhibits the particles from reaching short distances where the attractive van der Waals attractions are strong enough to cause aggregation. In view of the wide range of properties of different polymers, brushes can be adapted to different applications and are therefore quite useful. Of particular interest are materials where the grafted colloids are embedded in a polymer matrix.[2,7−18] These compounds may exhibit a combination of different properties, such as flexibility and toughness, which is difficult to obtain otherwise. In the compound material, the colloids must be well dispersed, and it is therefore unfortunate that long melt chains have the tendency of destabilizing the colloidal dispersion.[19−23] This phenomenon is strongly related to the wetting *autophobicity* of a polymer melt on a top of a polymer brush.[24−27] Both effects can be attributed to expulsion of free chains from within the brush. The object of this paper is to study in detail the stabilizing effect of an effective negative (attractive) Flory parameter ($\chi < 0$) for the interaction between grafted and mobile chains.[28]

A similar scenario occurs in mixtures of homopolymers and block copolymers. Homopolymers have a uniform molecular composition along the chain, while block copolymers consist of several blocks, the composition being uniform only within each block. Important examples are diblock copolymers, where two different polymers (denoted A and B) are tethered together at one point, and triblock copolymers, composed of three such blocks.[29] When the incompatibility between the different blocks is large enough, the different constituents segregate into A-rich and B-rich mesophases. The size of these mesophases is limited by the presence of the tethering points, which are concentrated at the interfaces between the different regions. In the strong segregation limit the width of these interfaces is small enough, and they can be modeled as a grafted surface. The situation can be further complicated by the addition of homopolymers.[30] The presence of homopolymer chains might destabilize the mesostructure in an analogous way to the destabilization of colloidal suspensions. On the other hand, these mesophases are important for many practical applications such as super-tough materials and optical devices.[31] These applications depend on our ability to keep two or more polymers with different mechanical or optical properties interconnected in a mesophase with a very typical structure and length scale. Here again, by choosing the appropriate interaction parameter, we will be able to stabilize the desired structure.

The examples described above demonstrate the industrial importance of understanding the properties of brushes in a polymer melt. Nevertheless, there are some interesting conceptual questions that are of interest from a theoretical point of view. Clearly, the properties of the brush depend on the grafting density, the chain length, the interactions between the grafted chains, and the interactions of the grafted chains with the surface. In addition, the properties of the solvent play an important role in determining the structure of the brush. Indeed, entropic effects that drive the chain interpenetration capacity scale as the inverse of the molecular weight whereas enthalpic contributions are proportional to the chain length. Thus, on top of the common distinction between good, poor, and Θ solvent conditions, the size of the solvent molecules is an additional important parameter since it affects the ability of the solvent molecules to penetrate the grafted layer. Special conditions occur when the solvent consists of long polymer chains, where both the size of the macromolecules and their connectivity come into play. The size of the macromolecule limits its ability to

† Current address: Department of Chemistry and Biochemistry, UCLA, 607 C. Young Dr. East, Los Angeles, CA 90095-1569.
‡ Current address: Matière Molle et Chimie, ESPCI, 10 rue Vauquelin, 75231 Paris Cedex 05, France.

10.1021/ma011351g CCC: $22.00
Published on Web 05/21/2002

penetrate the brush by reducing its translational entropy. We now introduce an enthalpic interaction in order to recover the ability of the large solvent chains to mix with the grafted ones. When exactly does one of these effects dominate over the other? And why do attractive enthalpic interactions lead to intersurface repulsion? As we shall see below, these questions are all related and will be discussed in detail.

In the current study we employ the continuous version of the self-consistent field (SCF) approach where the partition function of each polymer chain is calculated numerically under the assumption that interchain interactions can be described by an average field generated by all the chains (the so-called mean field).[32,33] In this approach the behavior of a polymer chain is described by a diffusion equation in an external field which depends (self-consistently) on the local polymer concentration. The self-consistent partial differential equation can then be solved numerically. In the lattice version of this method, which is usually called the multilayer Scheutjens−Fleer lattice model,[34,35] space is divided into layers parallel to the surface. Recursion relations which take into account both the connectivity of the chains and the Boltzmann weight associated with the polymer interactions then relate the occupation ratio of adjacent layers and can be solved numerically, e.g., by iterations.

We also use the simpler scaling theory of polymer brushes, initiated by de Gennes[1,2] and Alexander,[3] to study the structure of the isolated brushes. The scaling approach is based on the assumption that the structure of the brush can be described by only *one* length scale, namely, the size of the brush h. Numerical calculations indicate that the scaling approach is valid in various limiting regimes.[36,37] A more refined analytical approach is the so-called parabolic approximation,[5,6] where the statistical sum over all possible configurations of a grafted chain is replaced by its most probable (classical) path.[4] This approximation is valid for strongly stretched chains when the fluctuations around the classical path are small. It turns out that the resulting average potential felt by a single grafted chain must be a parabolic function of the distance from the surface. The monomer density profile in the brush can then be calculated from this average potential. If, for example, monomer−monomer interactions inside the brush can be described by a second virial coefficient, the density profile is parabolic, being maximal near the surface and then decreasing continuously to zero. Because of its relative simplicity, the parabolic approximation was applied to a wide variety of systems.[5,6,9,28,38,39] The parabolic approximation breaks at the edge of the brush where fluctuations are important[8,40,41] and near the grafting surface where the repulsion of the from the hard surface creates a narrow depletion layer.[42] It was shown, however, that it becomes exact in the strong stretching limit, which is reached when the size of the brush is much larger than the ideal size of a polymer chain.[43−47]

The interaction between two brushes was studied theoretically,[48,49] experimentally,[50] and by computer simulations[51,52] and was found to be strongly repulsive due to the steric repulsion between the free ends ("tails") of the grafted chains. It should be noted that since the interactions between two polymer brushes strongly depend on the structure at the *edge* of the brush, the parabolic approximation can only give a very rough estimate of these forces.[49] In particular, interdigitation of the two brushes is totally neglected in this approach.

When the solvent is replaced by a polymer melt, the structure of the brush can change drastically.[2,7,9−13,15−18,24−27] Because of the large dimensions of the polymer chains, they are less likely to penetrate into the brush. In other words, it is easier to expel macromolecules from the brush because of their reduced entropy. The result is a dry brush, which contains no free polymers up to a small distance from the edge of the brush, as opposed to a wet brush, where the solvent molecules penetrate all the way through. The transition from a wet brush to a dry one depends strongly on the molecular weight of both grafted chains and the free ones and on the grafting density. If the solution contains small solvent molecules in addition to mobile polymers, the structure will depend also on the volume fraction of polymer in the solution.[13,21]

An important consequence of the large molecular weight of the mobile chains is the existence of attractive interactions between two brushes immersed in a polymer melt.[19−23] This attraction exists only between dry brushes in a high molecular weight solvent and can lead to destabilization of a suspension of grafted colloids embedded in a polymer melt. In a previous study,[28] we have used the strong stretching ("parabolic") approximation to show that by choosing a favorable interaction between the grafted and the free chains we can control the structure of the brush and the interbrush interactions. More specifically, if the Flory interaction parameter χ between the two species is negative, the grafted chains will extend into the polymer melt while the free chains will penetrate into the brush. The resulting wet brushes well repel each other, and the colloidal solution will be stabilized. In this study we extend the discussion beyond the strong stretching limit by solving the full SCF equations of the grafted and free chains. In addition, we present a detailed scaling picture of a single brush in contact with a polymer melt.

In the next section the scaling results for a single brush in contact with a polymer melt are reviewed and extended to include a negative χ parameter. In section III the full SCF equations are solved for the concentration profiles and the interbrush interactions. Some simple analytical approximations are provided as well. Finally, in the last section we present our conclusions and some points that require further investigations.

II. A Single Brush in a Polymer Melt

In this paper we study the interactions between colloids covered with a grafted layer and immersed in a polymer melt (Figure 1a). As we shall see below, the range of these interaction is of the order of the size of the brush h. Since in many practical cases the radius of the colloids R is much larger than h, the Derjaguin approximation[53] can be used to relate the interaction between flat surfaces (Figure 1b) to that of two large spheres.

At the onset of interaction, the structure of the two brushes resembles an isolated brush in contact with a polymer melt. This initial state is an important factor in determining the nature of the interbrush interactions, and it is therefore important to understand first the structure of a single brush.

The discussion in this section is limited to simple scaling arguments, which describe accurately the general behavior but leave out the numerical prefactors.

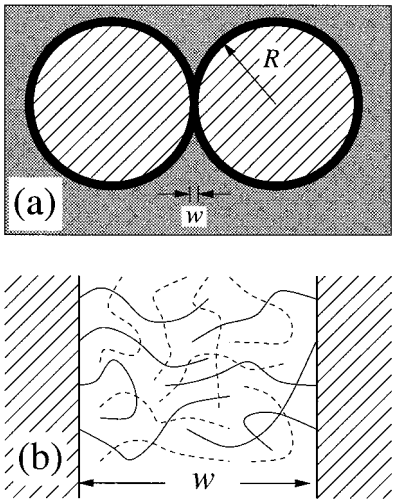

Figure 1. (a) Schematic view of two spherical particles of radii R immersed in a polymer melt of free chains. A layer of grafted polymer chains covers the particles. The distance between the two surfaces w is much smaller than their radii. (b) Schematic view of two interacting brushes (solid lines) immersed in a polymer melt of free chains (dashed lines). The grafted surfaces are flat and placed at a distance w from each other.

The physical parameters that are associated with the brush are the index of polymerization of the grafted chains N and the grafting density σ/a^2 (number of grafted chains per unit area), where a is the size of a monomer. For simplicity and clarity, the same monomer dimensions are assumed for both grafted and free chains. Furthermore, the same molecular volume, a^3, is assigned to the monomers of the two species.

The parameters associated with the free chains are the index of polymerization P and the monomer concentration in the melt $\rho_0 = 1/a^3$. Because of the incompressibility of the mixed polymer system, the total concentration is fixed everywhere:

$$\rho_N(\mathbf{r}) + \rho_P(\mathbf{r}) = \rho_0 \tag{1}$$

where $\rho_N(\mathbf{r})$ and $\rho_P(\mathbf{r})$ are the local monomer concentrations of the grafted ("N") chains and the free ("P") chains, respectively. At low molecular weights the melt becomes a regular solvent.

The short-range interaction between monomers of the grafted chains and the mobile chains can be characterized by the Flory interaction parameter χ characterizing the effective enthalpic interaction energy of one monomer from the grafted species with another monomer from the mobile species in units of k_BT, k_B being the Boltzmann constant and T the temperature. The value of χ is determined by the structure of the monomers on the atomic level and represents the overall contribution of several sources, such as induced dipole moments, differences in dielectric constants, packing constraints, etc. In the most general case χ depends also on the local composition, but this dependence will be neglected in the following arguments.

Three different cases can be distinguished depending on the sign of χ. The simplest and most intensively studied case is that of chemically identical molecules ($\chi = 0$), for which detailed diagrams of states where constructed.[2,9,13,15,18] The case of incompatible polymers ($\chi > 0$) is a generalization of poor solvent conditions where mixing of the grafted and free chains is discouraged. The grafted layer is therefore collapsed and does not penetrate into the solution.[11] The case of compatible polymers ($\chi < 0$) is a generalization of good solvent conditions where the grafted chains are encouraged to mix with free chains and the chains stretch further away from the grafting surface.[7,12] For most polymer mixtures χ is positive, but in some cases specific interactions (e.g., dipole−dipole or hydrogen bridging) may lead to negative (attractive) values of χ. Typical examples include poly(methyl methacrylate) (PMMA)/poly(vinyl chloride) (PVC) blends[54] and poly(styrene) (PS)/poly(2,6-dimethyl-1,4-phenylene oxide) (PXE).[55] The negative χ case is the focus of this study; however, for comparison and clarity a short review of the $\chi = 0$ case is presented.

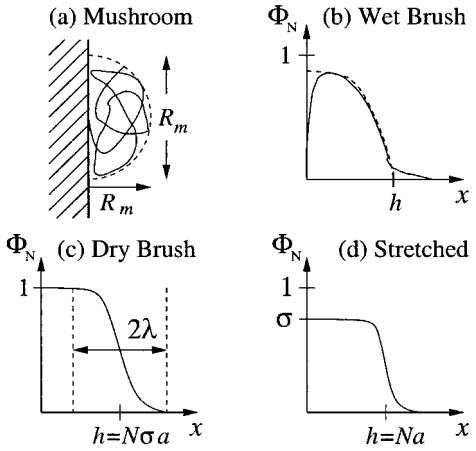

Figure 2. Three main structures of a brush: (a) schematic view of an isolated brush (mushroom). The envelope of the volume occupied by the chain is more or less a spherical cap of radius R_m. (b) Typical profile of a wet brush of width h. The dotted curve is the parabolic profile while the solid curve is the more realistic profile which includes the exponential tail at the edge of the brush and the depletion layer near the surface. (c) Typical profile of a dry brush. The width of the brush is $h \cong N\sigma a$, while the width of the interfacial layer is 2λ. In (b) and (c) the volume fraction of the brush $\phi_N(x)$ is plotted as a function of the distance x from the grafting surface. (d) Schematic view of a fully stretched brush. The width of the brush is $h = Na$ while the volume fraction is $\Phi_N = \sigma$.

1. Chemically Identical Polymers: $\chi = 0$.[2,9,13,15,18] In the absence of enthalpic interactions the structure of the brush depends on three parameters, namely N, P, and σ.[56] The different structures that can occur are shown schematically in Figure 2 while the corresponding diagram of states is presented in Figure 3. The following scaling regimes can be distinguished:

(1a) Swollen Mushrooms. At low grafting densities the grafted chains are isolated from each either and form a kind of a "fluffy" semispherical cap of radius R_m, resembling a mushroom. In a low molecular weight solvent the entropy of the solvent molecules contributes to an effective repulsion between the monomers on the grafted chain, which is of the order of a^3/P. The free energy of a single mushroom can be written as

$$F \cong \frac{R_m^2}{Na^2} + \frac{a^3}{P}\frac{N^2}{R_m^3} \tag{2}$$

where the first term is the elastic energy of the chain while the second term is the entropic excluded-volume contribution. In eq 2 and in the following all energies will be given in units of k_BT. Minimization with respect to R_m gives $R_m/a \cong N^{3/5}/P^{1/5}$.

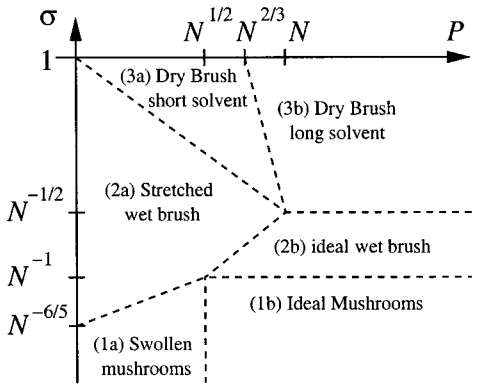

Figure 3. Diagram of states for grafted polymer (index of polymerization N) in contact with a chemically identical polymer melt (index of polymerization P). The grafting density is σ/a^2, a being the monomer dimension.

(1b) Ideal Mushrooms. The entropic excluded volume becomes of order $1k_BT$ when $P \cong N^{1/2}$. For higher values of P this contribution is negligible, the grafted chain is ideal, and $R_m/a \cong N^{1/2}$.

(2a) Stretched Wet Brush. The swollen mushrooms start to overlap when $\sigma/a^2 \cong 1/R_m^2$, corresponding to a reduced grafting density of $\sigma \cong P^{2/5}/N^{6/5}$. Above that value the grafted chains form a single layer near the surface in which the free energy per chain is

$$F \cong \frac{h^2}{Na^2} + \frac{a^3}{P}\frac{N^2}{ha^2/\sigma} \tag{3}$$

The first term is the elastic energy required to stretch the chain up to a distance h from the surface. The second term is the effective excluded-volume term where the volume per grafted chain is now $V_1 \cong ha^2/\sigma$ instead of R_m^3. Minimization of eq 3 with respect to h gives the size of the grafted layer, $h/a \cong \sigma^{1/3}N/P^{1/3}$.

(2b) Ideal Wet Brush. Similarly, ideal mushrooms begin to overlap when $\sigma \cong 1/N$. Since the entropic excluded volume is too weak, the width of the brush is the size of an ideal chain $h/a \cong N^{1/2}$. The crossover between the stretched wet brush (2a) and the ideal wet brush (2b) is when the entropic excluded-volume interaction (second term in eq 3) is of the order of $1k_BT$. This happens when $\sigma \cong P/N^{3/2}$.

(3a) Dry Brush, Short *P* Chains.[57] At even higher grafting densities, the volume fraction of grafted chains in the brush V_1/Na^3 becomes of order unity. In the case of a stretched wet brush this corresponds to $\sigma \cong 1/P^{1/2}$. The volume fraction inside the brush is unity up to a layer of thickness λ, which is the penetration length of the mobile molecules into the brush. From packing constraints the size of the brush is given by $h \cong N\sigma a$ while the penetration length can be obtained from the following free energy per unit area:

$$F \cong F_{el} + F_{short} \cong \frac{\sigma}{a^2}\frac{\lambda^2}{Na^2} - \lambda\frac{a^3}{P}\left(\frac{1}{a^3}\right)^2 \tag{4}$$

The first term is the elastic response of the brush to stretching by an additional amount λ.[30] The second term is the entropic gain of allowing the solvent molecules to penetrate into a layer of width λ. Minimizing the free energy with respect to λ gives $\lambda \cong N/\sigma P$. Note that the dry brush becomes a wet brush when the penetration length is comparable to the size of the brush, $\lambda \cong N\sigma a$.

(3b) Dry Brush, Long *P* Chains. In the ideal wet brush regime (2b) the volume becomes of the order unity when $\sigma \cong 1/N^{1/2}$. The size of the brush is again $h \cong N\sigma a$, but the penetration length follows a different scaling law. The reason is that for large values of P the entropy of the large molecules is negligible while the connectivity of the solvent polymer chains becomes important. The contribution of the connectivity of the chain to the free energy per unit area is

$$F_{long} \cong \int dx \frac{a^2}{\rho_P(x)}|\rho'_P(x)|^2 \cong \frac{1}{\lambda a} \tag{5}$$

where the local concentration of the free chains $\rho_P(x)$ varies from $1/a^3$ in the polymer melt to zero inside the brush over a length scale λ. The competition between this term and the first term of eq 4 yields $\lambda \cong N^{1/3}/\sigma^{1/3}$. Note that for large values of the solvent polymerization index P the results are always independent of P. The crossover between small molecule behavior and large molecule behavior is obtained when F_{el} (eq 4) is comparable to F_{long} (eq 5), yielding $\sigma \cong N/P^{3/2}$.

2. Compatible Polymers: $\chi < 0$. The above arguments can be now generalized to include a short-range enthalpic attraction between the free chains and the grafted ones. This attraction is represented by a negative Flory parameter $\chi < 0$. While the entropy of the free chains scales as $1/P$ and therefore dominates for short chains, the enthalpic interaction is proportional to χP and is therefore dominant for long chains. Enthalpic effects will therefore appear first in the right-hand side of the diagram of states (Figure 3) and then, as the interaction becomes stronger, move progressively to the right. The borderline between the entropy-dominated regimes and the enthalpy-dominated regimes is approximately at $|\chi|P \cong 1$.

As long as $|\chi| < 1/N$, the enthalpic interaction is too weak to affect the structure of the brush and the diagram (Figure 3) is unaffected. At higher magnitudes the diagram of states changes gradually as depicted in Figure 4. The effect on the brush structure is also depicted in Figure 5 for long solvent molecules ($P \geq N$, right-hand side of Figure 3). Several new scaling regimes appear:

(3c) Enthalpic Dry Brush. In the dry brush regime, the brush and the P chains interact only in the interfacial layer whose thickness is of order λ. The contribution of this interaction to the free energy per unit area is therefore

$$F_{int} \cong \chi a^3 \int dx\, \rho_N(x)\, \rho_P(x) \cong -|\chi|\frac{\lambda}{a^3} \tag{6}$$

For long chains (regime 3b) this term becomes comparable to the gradient term F_{long} (eq 5) when

$$\sigma \cong N|\chi|^{3/2} \tag{7}$$

This crossover grafting density becomes of order unity when

$$|\chi| \cong 1/N^{2/3} \tag{8}$$

At higher values of $|\chi|$, regime 3b disappears, and the diagram shown in Figure 4a changes into the diagram of Figure 4b.

Returning to the enthalpic dry interacting brush (regime 3c), the penetration length λ is now determined

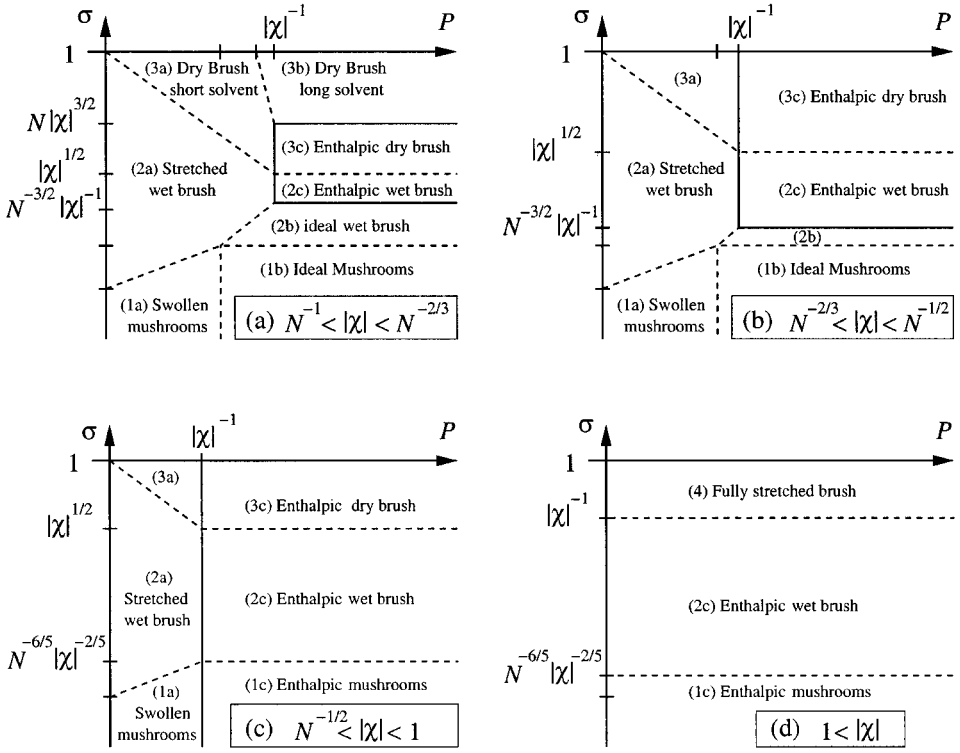

Figure 4. Diagrams of states for a brush in contact with a polymer melt. The four diagrams correspond to different values of χ, the Flory interaction parameter of the grafted chains with the free chains.

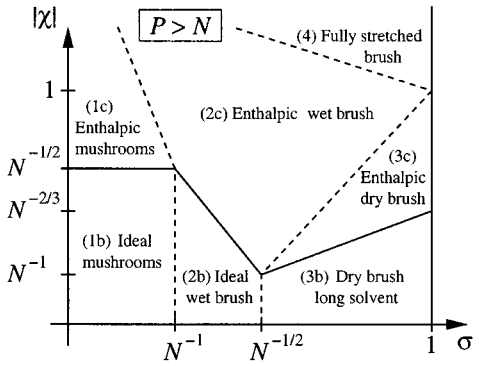

Figure 5. Diagram of states for a brush in contact with a polymer melt in the $\sigma-\chi$ plane. The diagram corresponds to the long solvent limit ($P \geq N$).

by the competition between the elastic energy F_{el} and the interaction energy F_{int}, yielding

$$\lambda \cong \frac{N|\chi|}{\sigma} \tag{9}$$

The crossover between this regime and the regime 3a (dry brush, short solvent) is reached when $F_{int} \cong F_{short}$. As expected, this happens when $|\chi|P \cong 1$.

(2c) Enthalpic Wet Brush. In the enthalpic dry brush the effect of lowering the grafting density is to increase the penetration length λ until the point where $\lambda \cong h$. The grafting density at this point is

$$\sigma \cong |\chi|^{1/2} \tag{10}$$

and it marks the crossover between the enthalpic dry brush and the enthalpic wet brush (see Figure 4a). For an enthalpic wet brush the free energy per chain reads

$$F \cong \frac{h^2}{Na^2} + a^3|\chi|\frac{N^2}{ha^2/\sigma} \tag{11}$$

The first term is the stretching energy of the chain while the second is the enthalpic contribution. This term is equivalent to an effective excluded-volume repulsion between monomers belonging to the grafted chains $v \cong |\chi|a^3$. Minimizing the above free energy with respect to the brush height h gives

$$h \cong \sigma^{1/3}|\chi|^{1/3}Na \tag{12}$$

The grafted chains are stretched as can be inferred from the fact that h is linear in chain length N. The chains become unstretched as soon as the enthalpic term in eq 11 is of the order of $1k_BT$. This point marks the crossover between the interacting wet brush (regime 2c) and the ideal wet brush (regime 2b). The crossover grafting density is

$$\sigma \cong \frac{1}{|\chi|N^{3/2}} \tag{13}$$

As the enthalpic interaction increases, the crossover grafting density decreases until the point where the upper boundary of the ideal wet brush (regime 2b) coincides with its lower boundary. This happens when

$$|\chi| \cong 1/N^{1/2} \tag{14}$$

and consequently the diagram depicted in Figure 4b becomes the diagram in Figure 4c.

(1c) Interacting Mushrooms. Consider now the effect of enthalpic interactions on an isolated mushroom.

The free energy of a single grafted chain can be written as

$$F \cong \frac{R_m^2}{Na^2} + a^3|\chi|\frac{N^2}{R_m^3} \tag{15}$$

where the second term represents the effective repulsion between monomers on the grafted chain as a result of the attraction between these monomers and the surrounding polymer melt. In fact, from the thermodynamic point of view the situation is equivalent to that of a grafted chain in a good solvent. The size of the mushroom, which is obtained by minimizing the free energy (eq 15) with respect to R_m, is

$$R_m \cong N^{3/5}|\chi|^{1/5}a \tag{16}$$

The interacting mushroom appears when the second term in eq 15 exceeds $1k_BT$. This happens for $|\chi| \geq 1/N^{1/2}$ where the interacting mushroom replaces the ideal mushroom. Incidentally, this crossover coincides with the disappearance of the ideal wet brush. Comparing the free energies of the swollen mushroom and the interacting mushroom, one is not surprised to find that the crossover between the two occurs for $P \cong 1/|\chi|$.

(4) Fully Stretched Brush. Finally, we note that as the magnitude of χ increases, the dry brush regimes shrink until they disappear completely from the diagram of states. This is due to the strong affinity of the grafted chains toward the free ones. Similarly, in the wet interacting brush, the grafted chains become more and more stretched until they reach their maximal length, $h_{max} = Na$ (see Figure 2d). Using eq 12, we find the maximal extensibility is obtained when the grafting density is

$$\sigma \cong \frac{1}{|\chi|} \tag{17}$$

At higher grafting densities the chains are highly stretched, and the average concentration in the brush is constant, as for a dry brush. On the other hand, since the volume fraction in the brush is smaller than unity, the free chains fully penetrate the brush as for a wet brush. The new regime is indicated in Figure 4d.

The purpose of introducing the negative χ parameter was to overcome the attraction between two brushes in a long polymer melt.[19−23] This attraction appears when the two brushes are in the dry brush, long solvent regime (regime 3b). As demonstrated by the arrow in Figure 5, when enthalpic interactions are included, the dry brush will become a wet brush, where interbrush interactions are expected to be repulsive. This is indeed verified in the next section.

III. Two Interacting Brushes

We now proceed to study the effect of the brush structure on the interactions between two grafted layers. We use a self-consistent-field formalism to calculate numerically the concentration profiles and the intersurface interactions. The formalism will be briefly reviewed in order to clarify the underlying assumptions and approximations present in this approach.

1. The SCF Formalism. Our model system consists of two flat parallel surfaces at a distance w from each other (see Figure 1b). Each surface carries M_N end-grafted chains of index of polymerization N at an average grafting density σ/a^2. In addition, the volume between the surfaces contains M_P free chains of index of polymerization P. The free chains can exchange freely with a reservoir of polymer chains where the volume fraction of polymer chains is $\phi_0 = 1$ and the chemical potential is $\mu_0 = \ln(\phi_0/P)$ in units of k_BT.

The partition function of the system can be expressed as a multiple of path integrals over the positions of monomers belonging to the grafted and free chains:

$$Z = \frac{1}{(M_N!)^2}\sum_{M_P=1}^{\infty}\frac{e^{M_P\mu_0}}{M_P!} \times \int D\mathbf{r}_{l_1}\exp\left(-\frac{3}{2a^2}\sum_{l_1=1}^{M_N}\int_0^N \dot{\mathbf{r}}_{l_1}^2\,ds\right) \times \int D\mathbf{r}_{l_2}\exp\left(-\frac{3}{2a^2}\sum_{l_2=1}^{M_N}\int_0^N \dot{\mathbf{r}}_{l_2}^2\,ds\right) \times \int D\mathbf{r}_{l_P}\exp\left(-\frac{3}{2a^2}\sum_{l_P=1}^{M_P}\int_0^P \dot{\mathbf{r}}_{l_P}^2\,ds\right) \times \exp\left(-\int V(\hat{\rho}_N,\hat{\rho}_P)\,d\mathbf{r}\right) \tag{18}$$

where $l_1 = 1, ..., M_N$, $l_2 = 1, ..., M_N$, and $l_p = 1, ..., M_p$ are the indices of the individual chains and s is the continuous contour index along the chains, $s \in [0,N]$ ($s \in [0,P]$) for the grafted (free) chains. The partition function is canonical with respect to the grafted chains (fixed amount) and grand canonical with respect to free chains as indicated by the chemical potential term. The three Gaussian terms associated with the integrals over the monomer positions are the standard Wiener measures of a three-dimensional random walk.[58] The interaction term $V(\mathbf{r})$ can be expressed in terms of the local monomer concentrations as

$$V(\mathbf{r}) = -\frac{a^3}{2\kappa}(\rho_0 - \hat{\rho}_N - \hat{\rho}_P)^2 + \chi\hat{\rho}_N\hat{\rho}_P \tag{19}$$

where the first term represents the compressibility of the polymer mixture. Typically, the compressibility of polymer melts is small and in practice $\rho_N(\mathbf{r}) + \rho_P(\mathbf{r}) = \rho_0$ throughout the system. The second term is the enthalpic interaction contribution ($\chi < 0$). The local concentrations of grafted and free monomers are given by

$$\hat{\rho}_N(\mathbf{r}) = \sum_{l_1=1}^{M_N}\int_0^N \delta[\mathbf{r} - \mathbf{r}_{l_1}(s)]\,ds + \sum_{l_2=1}^{M_N}\int_0^N \delta[\mathbf{r} - \mathbf{r}_{l2}(s)]\,ds \tag{20}$$

$$\hat{\rho}_P(\mathbf{r}) = \sum_{l_P=1}^{M_P}\int_0^P \delta[\mathbf{r} - \mathbf{r}_{l_P}(s)]\,ds \tag{21}$$

It is now convenient to introduce two pairs of collective coordinates in the partition function through the definition of the δ function

$$1 = \int D\rho_i(\mathbf{r})\,\delta[\rho_i(\mathbf{r}) - \hat{\rho}_i(\mathbf{r})] = \int D\rho_i(\mathbf{r})\int D\varphi_i(\mathbf{r})\exp\left(\int i\varphi_i(\mathbf{r})[\rho_i - \hat{\rho}_i]\,d\mathbf{r}\right) \tag{22}$$

where $i = N, P$. This transformation introduces the monomer number densities ρ_N and ρ_P and their conju-

gated fields φ_N and φ_P. The partition function can then be expressed in terms of these densities and fields as

$$Z = \int D\rho_N D\rho_P D\varphi_N D\varphi_P \frac{\zeta_1^{M_N}}{M_N!}\frac{\zeta_2^{M_N}}{M_N!} \exp(e^{\mu_0}\zeta_P) \times \exp(-\int V(\rho_N,\rho_P)\, d\boldsymbol{r} + \int i\varphi_N(\boldsymbol{r})\, \rho_N\, d\boldsymbol{r} + \int i\varphi_P(\boldsymbol{r})\, \rho_P\, d\boldsymbol{r}) \quad (23)$$

where $\zeta_1[i\varphi_N]$ and $\zeta_2[i\varphi_N]$ are the partial partition functions of a single chain grafted to the first and second surface, respectively. The external field $i\varphi_N$ carries the influence of all the other chains (free as well as grafted). Similarly, $\zeta_P[i\varphi_P]$ is the partial partition function of a free polymer chain in the external field $i\varphi_P$. More specifically,

$$\zeta_i = \int D\boldsymbol{r}(s) \exp\left(-\int_0^N \left\{\frac{3}{2a^2}\dot{\boldsymbol{r}}^2 + i\varphi_N[\boldsymbol{r}(s)]\right\} ds\right) \quad i = 1, 2 \quad (24)$$

$$\zeta_P = \int D\boldsymbol{r}(s) \exp\left(-\int_0^P \left\{\frac{3}{2a^2}\dot{\boldsymbol{r}}^2 + i\varphi_P[\boldsymbol{r}(s)]\right\} ds\right) \quad (25)$$

On a mean field level the partition function eq 23 is approximated by replacing the path integrals over the densities and the fields with their values at the saddle point of the integrand. The free energy of the system is then

$$F = \int \{V(\rho_N,\rho_P) - w_N(\boldsymbol{r})\rho_N - w_P(\boldsymbol{r})\rho_P\}\, d\boldsymbol{r} + M_N[\ln M_N/\zeta_1 - 1] + M_N[\ln M_N/\zeta_2 - 1] - e^{\mu_0}\zeta_P \quad (26)$$

The average number densities ρ_N and ρ_P and the average (mean) fields $w_N = i\varphi_N$ and $w_P = i\varphi_P$ are given by the variational equations $\delta F/\delta\rho_N = 0$, $\delta F/\delta\rho_P = 0$, $\delta F/\delta w_N = 0$, and $\delta F/\delta w_P = 0$. The first pair of equations relates the mean fields felt by the grafted and the free to the average densities:

$$w_N = -\frac{a^3}{\kappa}(\rho_0 - \rho_N - \rho_P) + \chi a^3 \rho_P \quad (27)$$

$$w_P = -\frac{a^3}{\kappa}(\rho_0 - \rho_N - \rho_P) + \chi a^3 \rho_N \quad (28)$$

The mean potentials $w_N(\boldsymbol{r})$ and $w_P(\boldsymbol{r})$ represent the energy required to insert an additional monomer belonging to a grafted or free chain, respectively, at a position $\boldsymbol{r}$. For low values of κ, the first terms in eqs 27 and 28 ensure incompressibility. The second term is the enthalpic coupling of the two chemical species.

The second pair of variational equations relates the monomer number densities to derivatives of the single chain partition functions. The latter can be expressed in terms of the polymer propagator functions.[33,59] Neglecting inhomogeneieties in the direction parallel to the grafting surfaces, the monomer concentrations in the confined system ($0 \le x \le w$) are

$$\rho_N(x) = \rho_1(x) + \rho_2(x) \quad (29)$$

where

$$\rho_j(x) = \frac{\sigma}{a^2}\frac{\int_0^N q_j(x,s)\, q_j^*(x,N-s)\, ds}{\int_0^w q_j(x,N)\, dx} \quad j = 1, 2 \quad (30)$$

and

$$\rho_P(x) = \frac{\phi_0}{Pa^3}\int_0^P q_P(x,s)\, q_P(x,P-s)\, ds \quad (31)$$

The forward propagator functions $q_1(x,s)$ and $q_2(x,s)$ are proportional to the probability of a chain segment grafted to the first or second surface, respectively, to reach a point x after s steps. The backward propagator functions $q_1^*(x,N-s)$ and $q_2^*(x,N-s)$ represent the rest of the grafted chain ("tail") starting anywhere between the two surfaces and connecting to the grafted segment at position x following $N-s$ steps. These four functions are determined by solving the following diffusion equation

$$\frac{\partial q(x,s)}{\partial s} = \frac{a^2}{6}\frac{\partial^2 q(x,s)}{\partial x^2} + w_N(x)\, q(x,s) \quad (32)$$

with the following initial conditions:

$$q_1(x,0) = \delta(x), \quad q_2(x,0) = \delta(w-x) \quad (33)$$

$$q_1^*(x,0) = 1, \quad q_2^*(x,0) = 1 \quad (34)$$

The first couple of initial conditions reflect the fact that the first ($s = 0$) monomer is attached to the surface while the second couple reflects the fact that the free ends of the grafted chains are a priori unbiased with respect to their initial position.

In the case of the free chains the forward and backward propagators are both unbiased and are therefore identical. The corresponding diffusion equation and boundary conditions read

$$\frac{\partial q_P(x,s)}{\partial s} = \frac{a^2}{6}\frac{\partial^2 q_P(x,s)}{\partial x^2} + w_P(x)\, q_P(x,s) \quad (35)$$

$$q_P(x,0) = 1 \quad (36)$$

The boundary conditions for the propagators are the same for all the propagators and reflect the impenetrability of the grafting surfaces to all polymer species:

$$q(x,s) = 0 \quad \text{for } x < 0 \text{ or } x > w \quad (37)$$

The symmetry of the system with respect to the midplane $x = w/2$ is such that $q_1(x,s) = q_2(w-x,s)$ and $q_1^*(x,s) = q_2^*(w-x,s)$. We are therefore left with three diffusion equations for three propagators $q_1(x,s)$, $q_1^*(x,s)$, and $q_P(x,s)$. These equations are coupled to each other through the dependence of the self-consistent fields $w_N(x)$ and $w_P(x)$ on the local monomer densities $\rho_N(x)$ and $\rho_P(x)$. This system of equations can be solved numerically by iterations after discretizing space, e.g., at intervals $\Delta x = a$ and the chain contour at intervals $\Delta s = 1$ (see for example ref 60). The criterion for numerical stability for an explicit finite difference algorithm is

$$\Delta x^2/\Delta s > a^2/6 \quad (38)$$

2. Interaction Free Energies. Once the self-consistent-field equations are solved, the excess free energy of interaction per unit area between the two surfaces can be calculated from eq 26. The interaction free energy per unit area then becomes

$$f_{\mathrm{pol}}(w) = \int \left\{ \frac{a^3}{2\kappa}[\rho_0 - (\rho_N + \rho_P)^2] - \chi\rho_N\rho_P \right\} \mathrm{d}x + 2\frac{\sigma}{a^2}[\ln(\sigma/\int_0^w q_1(x,N)\,\mathrm{d}x) - 1] \quad (39)$$

where the coupling of the free chains to a reservoir was taken into account.

Equation 39 contains only the polymer contribution to the free energy. In practical systems these interactions compete with the attractive van der Waals interactions.[53] In the discussion below only nonretarded forces will be considered as they are of longer range than the retarded forces. The nonretarded van der Waals interactions between two flat surfaces denoted (1) and (3) at a distance w from each other across media (2) can be approximated by

$$f_{\mathrm{vdW}}(w) = \frac{A_{123}}{12\pi w^2} \quad (40)$$

where A_{123} is the Hamaker constant and has units of energy. A relatively simple approximation for the Hamaker constant is given by[53,61]

$$A_{123} = \frac{3}{4}\frac{(\epsilon_1 - \epsilon_2)(\epsilon_2 - \epsilon_3)}{(\epsilon_1 + \epsilon_2)(\epsilon_2 + \epsilon_3)} + \frac{3}{8\sqrt{2}}\frac{2\pi\hbar\nu}{k_{\mathrm{B}}T} \times \frac{(n_1^2 - n_2^2)(n_2^2 - n_3^2)}{\sqrt{n_1^2 - n_2^2}\sqrt{n_2^2 - n_3^2}(\sqrt{n_1^2 - n_2^2} + \sqrt{n_2^2 - n_3^2})} \quad (41)$$

The first term is the static contribution of induced dipole−dipole interactions, ϵ_1, ϵ_2, and ϵ_3 being the static dielectric constants of the different media. The second term is the dispersion energy due temporal correlations between induced dipole moments, n_1, n_2, and n_3 being the refractive indices of the different media, $\hbar$ is the Planck constant, and ν is the first resonance frequency, taken to be the same for the different media. Typically, $\nu \cong 3 \times 10^{15}$ Hz and $2\pi\hbar\nu \cong 480 k_{\mathrm{B}}T$. In aqueous solutions the high dielectric constant of water leads to values of the Hamaker constant of the order of 10^{-20} J. On the other hand, if the dielectric constants of the three media are of the same order of magnitude, as is often the case in polymer blends, the second term will dominate the Hamaker constant A_{123}. The corresponding Hamaker constant is lower, of the order of 10^{-21}–10^{-20} J.

In the dry brush regime the interface between the brush and the polymer melt is relatively sharp provided that $\lambda \ll h$. In this case, five distinct layers should be considered: the two colloid surfaces (1), two brushes (2), and the polymer melt (3). The van der Waals interaction energy of such geometry can be approximated by[53,61]

$$f_{\mathrm{vdW}}(w) = \frac{1}{12\pi}\left[\frac{A_{232}}{(w - 2h)^2} - \frac{2A_{123}}{(w - h)^2} + \frac{A_{121}}{w^2}\right] \quad (42)$$

It follows from eq 41 that the two terms A_{121} and A_{232} are negative while the sign of A_{123} depends on the relation between the dielectric properties of the three materials. When the two brushes approach each other, the first term dominates and the interaction will be attractive. When the two brushes start to overlap, the sharp brush/melt interface disappears and only the last term in eq 42 will remain, where medium (2) is replaced by an effective medium consisting of both grafted and free chains.

When the dry brush is replaced by a wet brush, two effects lead to a reduction in the destabilizing effect of the van der Waals interactions. First, in the wet brush the mobile polymer chains are present inside the brush, and the concentration profile changes gradually between the surface and the polymer melt. Consequently, the sharp brush/melt boundary does not exist anymore, and the two first terms in eq 42 becomes irrelevant. Second, the width of a wet brush is larger than the size of a dry brush. The van der Waals interactions scale as $1/w^2$ and are therefore much weaker at the point where the two brushes start to overlap, and the nature of the inter-brush interactions is determined by the bare polymeric interactions.

Finally, the grafted colloids are typically spherical particles. When their radius R is much larger than the typical size of the brush (namely, $R \gg h$), the interparticle interaction energy $U_R(w)$ can be calculated from the interaction free energy of two flat surfaces $f_{\mathrm{tot}}(w) = f_{\mathrm{pol}}(w) + f_{\mathrm{vdW}}(w)$ using the Derjaguin approximation:[53]

$$U_R(w) = \pi R \int_w^\infty f_{\mathrm{tot}}(w')\,\mathrm{d}w' \quad (43)$$

IV. Results and Discussion

In this section the effect of enthalpic interactions is studied numerically by solving the SCF equations described above. We start by considering the structural change of a single brush as a result of enthalpic interactions. In Figure 6 the effect of the Flory parameter χ on the brush volume fractions profiles is illustrated at moderate ($\sigma = 0.1$) and high ($\sigma = 0.3$) grafting densities (Figure 6, a and b, respectively). At the chain length used ($N = 100$) a grafting density of $\sigma = 0.1$ (Figure 6a) places the brush at the crossover between the dry brush regime and the wet brush regime (see schematic diagram in Figure 5). At high grafting densities (Figure 6b) the effect is more pronounced and follows the arrow drawn in Figure 5. In the absence of enthalpic interactions the free chains are expelled from the brush, and the volume fraction is unity throughout most of the brush. Indeed, the width of the brush is $h/a \cong N\sigma = 30$, in agreement with the dry brush regime. In the presence of weak enthalpic interactions ($\chi = -0.15$) the brush slightly swells but remains in the enthalpic dry brush regime. Finally, at high values of χ the enthalpic wet brush regime is reached, where free chains penetrate all the way into the brush.

When two grafted surfaces are drawn closer to each other, the composition and structure of the polymer blend located between the two surfaces change as depicted in Figure 7. As soon as the brushes start to overlap free chains must be expelled from the gap because of the melt incompressibility. At the same time the grafted chains are squeezed together as they are confined to slit smaller than their natural size $w < 2h$. These two processes are demonstrated in Figure 7 where the volume fraction profiles are plotted for several inter-surface separations.

In Figure 7a, a sequence of concentration profiles is depicted for two interacting dry brushes ($N = P = 100$,

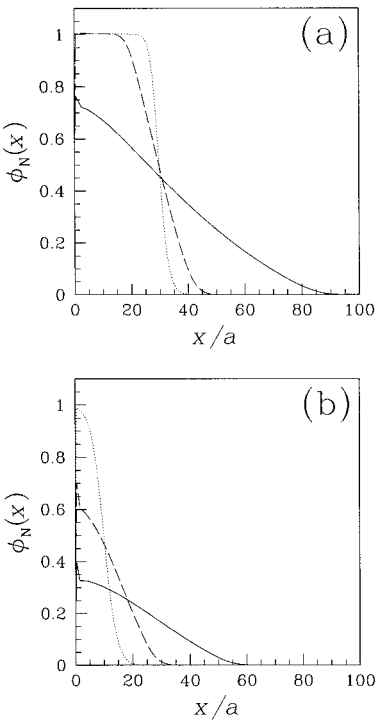

Figure 6. Brush volume fraction $\phi_N(x)$ as a function of the reduced distance x/a from the grafting surface for three values of χ. The different curves correspond to $\chi = 0$ (solid line), $\chi = -0.15$ (dashed curve), and $\chi = -0.5$ (dots). The polymerization indices of the grafted and free chains are $N = P = 100$, and the reduced grafting density is $\sigma = 0.3$ (a) and $\sigma = 0.1$ (b). Incompressibility was ensured by taking $\kappa = 0.01$.

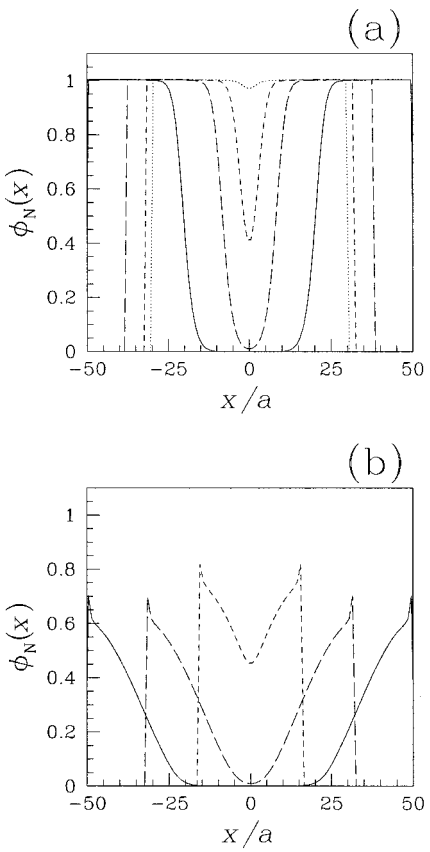

Figure 7. Brush volume fraction $\phi_N(x)$ between two grafting surfaces for several separations w. (a) In the absence of enthalpic interactions ($\chi = 0$, $\sigma = 0.3$) and (b) in the presence of enthalpic interactions ($\chi = -0.15$, $\sigma = 0.1$). The different curves correspond to $w = 120a$, $w = 70a$, $w = 62a$ (a) and to $w = 120a$, $w = 95a$ (b). The profiles are depicted so that the mid-planes coincide at $x = 0$ and the surfaces are located at $x = \pm w/2$. The physical parameters are $N = P = 100$ and $\kappa = 0.01$.

$\sigma = 0.3$, $\chi = 0$), while in Figure 7b the two brushes are in the enthalpic wet brush regime ($N = P = 100$, $\sigma = 0.1$, $\chi = -0.15$). The concentration profiles are accompanied by the end-point distribution of the grafted chains $q_1(x,N)$ plotted in Figure 8 for the same profiles of Figure 7. As the two surfaces are brought closer together, the end points are squeezed toward the mid-plane. While the end-point distribution is quite narrow in the dry brush regime, it is much wider in the wet brush regime and therefore much more influenced by the presence of the second brush.

The two effects mentioned above are important for understanding the nature of the intersurface interactions as plotted in Figure 9. For chemically identical grafted and free chains attraction can be observed at overlap separations. This attraction can be understood by looking at the interpenetration length λ between free and grafted chains into the brush. In the dry brush regime the volume fraction of a single brush is well described by a hyperbolic tangent profile[30]

$$\phi_N(x) = 1 - \phi_P(x) = \frac{1}{2}\left[1 - \tanh\left(\frac{x-h}{\lambda}\right)\right] \quad (44)$$

where $h = N\sigma a$. The elastic contribution to the free energy is then given by

$$f_{el} = \frac{1}{24a}\int_0^\infty \left\{\frac{1}{\phi_N}|\nabla\phi_N|^2 + \frac{1}{\phi_P}|\nabla\phi_P|^2\right\} \cong \frac{1}{12\lambda a} \quad (45)$$

The brush stretching energy due to interpenetration can be estimated using the parabolic approximation.[30] For a dry brush the volume fraction profile has a boxlike distribution (i.e., $\phi_N(x)$ is unity for $0 \le x \le h$ and zero otherwise), and the potential felt by the grafted chains is parabolic: $w_N(x) = B(h^2 - x^2)$ where $B = 3\pi^2/8N^2a^2$.[5,6,9,21] The excess stretching free energy can therefore be estimated by comparing the potential energy of the interpenetrating state as described by eq 44 with the energy of the box like distribution. Linearizing $w_N(x)$ around $x = h$ yields

$$f_{pen} = -\frac{1}{a^3}\int_0^h w_N(x)[\phi_N(x) - 1] - \frac{1}{a^3}\int_h^\infty w_N(x)[\phi_N(x) - 0] \cong \frac{\pi^4\sigma\lambda^2}{32Na^4} \quad (46)$$

Minimizing now the total free energy of a dry brush with long solvent molecules (regime 3b) $f_{long} = f_{el} + f_{pen}$ gives the optimal penetration length

$$\lambda_1 = \left(\frac{4}{3\pi^4}\right)^{1/3}\left(\frac{N}{\sigma}\right)^{1/3}a \quad (47)$$

and the total free energy is

$$f_{long}^{(1)} = \frac{1}{8\lambda_1 a} \quad (48)$$

When two dry brushes approach each other, the gradient term f_{el} can be reduced by increasing the mid-plane value of $\phi_N(x)$. Since the melt is incompressible, this increase is accompanied by further interpenetration

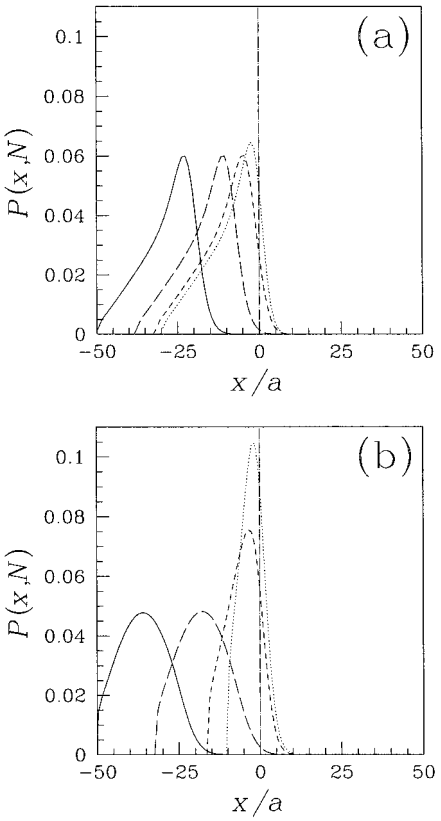

Figure 8. Renormalized end-point distribution $q_1(x,N)$ for the profiles depicted in Figure 7. Same notations and physical values as in Figure 7. The mid-plane ($x = 0$) is indicated by a vertical line.

of the free chains into the two brushes and an increase in λ. This can be seen semiquantitatively by the following argument. We assume that in the limit where the distance between the brush/melt interface $l = w - 2N\sigma a$ is much larger than λ the concentration profile can be described by the following trial function:

$$\phi_N(x) = \begin{cases} \frac{1}{2}\left[1 + \tanh\left(\frac{|x| - l}{\lambda}\right)\right] & l < |x| \le \frac{w}{2} \\ \cosh\left(\frac{2|x|}{\lambda}\right)\exp\left(-\frac{2l}{\lambda}\right) & -l < x \le l \end{cases} \quad (49)$$

Assuming that only the gradient term changes considerably, the free energy is now

$$f_{\text{long}}(w) \cong \frac{1}{6\lambda a}\left(1 - \frac{1}{2}e^{-4l/\lambda}\right) + \frac{\pi^4\sigma\lambda^2}{16Na^4} \quad (50)$$

The lowest order correction to λ is then

$$\lambda(w) \cong \lambda_1\left[1 + \left(\frac{4l}{\lambda_1} - 1\right)e^{-4l/\lambda}\right]^{1/3} \quad (51)$$

with

$$f_{\text{long}}(w) \cong \frac{1}{4\lambda a}\left[1 + \left(\frac{4l}{3\lambda} - 1\right)e^{-4l/\lambda}\right] \quad (52)$$

The resulting behavior is depicted in Figure 10 where the excess free energy of interaction $\Delta f_{\text{long}}(w) = f_{\text{long}}(w) - 2f^{(1)}_{\text{long}}$ is plotted as a function of l/a for $N = 100$ and $\sigma = 0.3$. The penetration length $\lambda(w)$ is plotted in the inset for the same physical parameters. Indeed, as soon as the two brushes start to overlap, the penetration

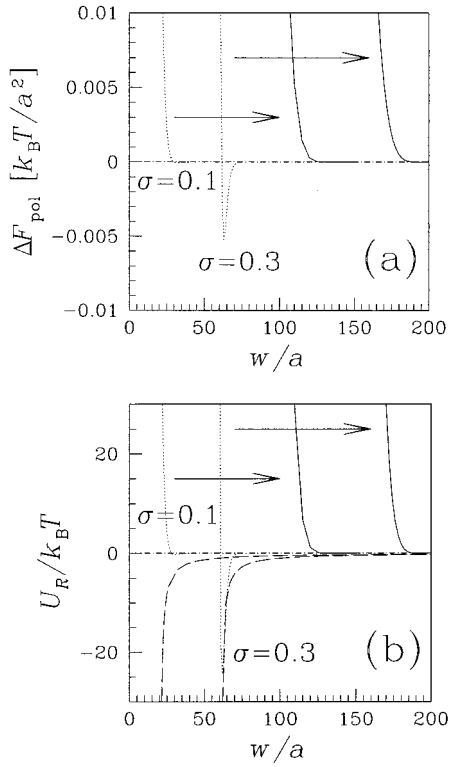

Figure 9. (a) Interaction free energy $f_{\text{pol}}(w)$ between two flat surfaces as a function of the reduced intersurface distance w/a. (b) Interaction potentials $U_R(w)$ of two brush-coated spherical particles of radius $R = 400a$ as a function of w/a. The different curves correspond to $\sigma = 0.1$ and $\sigma = 0.3$. The Flory parameter is $\chi = 0$ (dotted curves) and $\chi = -0.5$ (solid curves). The physical parameters are $N = P = 100$ and $\kappa = 0.01$. The arrows indicate the effect of changing the interaction parameter from $\chi = 0$ to $\chi = -0.5$. The dashed curves in (b) correspond to the van der Waals interactions between the two particles (eqs 41 and 42) with the following physical parameters: $\epsilon_1 = 2.3$, $n_1 = 1.5$ (polybutadiene rubber colloids), $\epsilon_2 = 3.6$, $n_2 = 1.5$ (grafted PMMA chains), $\epsilon_3 = 8.4$, $n_3 = 1.4$ (free PVDF chains), $\nu = 3 \times 10^{15}$ Hz, and $T = 300$ K.

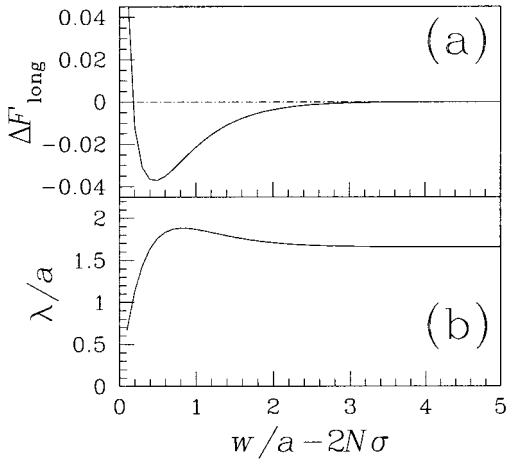

Figure 10. Excess free energy of interaction per unit area $\Delta f_{\text{long}}(w) = f_{\text{long}}(w) - 2f^{(1)}_{\text{long}}$ in units of k_BT/a^2 and penetration length $\lambda(w)$ (eqs 51 and 52) as a function of l/a for $N = 100$ and $\sigma = 0.3$.

length λ increases, leading to a decrease in the interaction free energy. The result is interbrush attraction, which is strong enough to destabilize grafted colloids in a polymer melt.[22]

This mechanism is absent whenever the brush becomes a wet brush. As discussed above, this can be

realized either by replacing the polymer melt with a low molecular weight solvent or by introducing attractive enthalpic interactions between the grafted and free chains. In the first case, the translational entropy of the solvent molecules pushes them to mix with the grafted chains, while in the latter case the driving force for mixing is enthalpic.

In the strong stretching limit (i.e., within the parabolic approximation) the molecular field can be written as $w_N = \nu\phi_N(x)$, where $\nu = 1/P$ for a low molecular weight solvent and $\nu = 2|\chi|$ when enthalpic interactions are present. The interbrush interactions are purely repulsive in this case and are given by[5]

$$\Delta f(w) \cong 2\left(\frac{\pi^2}{4}\right)^{1/3}\frac{\nu^{2/3}\sigma^{5/3}N}{a^2}\left[\frac{1}{2u}+\frac{u^2}{2}-\frac{u^5}{10}-\frac{9}{10}\right] \quad (53)$$

where $u = w/2h$ and

$$h \cong \left(\frac{4}{\pi^2}\right)^{1/3}\nu^{1/3}\sigma^{1/3}Na \quad (54)$$

In our case, fluctuations around the most probable path are important, and the validity of the strong stretching limit is quite limited. Nevertheless, the essential behavior is basically the same as can be seen in the results of the SCF calculations.

V. Conclusions

In this paper we have studied the effect of favorable enthalpic interactions ($\chi < 0$) on the structure and interactions of polymer brushes in contact with a polymer melt. Although negative χ parameters between different polymers are less common than positive ones, they play a crucial role in many applied systems.

First, the different scaling regimes of a single brush were analyzed. It was shown that enthalpic interactions could change the structure of the brush from a dry (collapsed) brush to a wet, (stretched) brush. In addition to scaling arguments, the self-consistent-field (SCF) method was used to study the structure of a brush and the interactions between polymer grafted colloids. It was shown that the structural change of the brush is accompanied by a prominent change in the nature of the interbrush interactions. More specifically, the well-established attractive intercolloidal interactions become repulsive, thus providing a simple mechanism for stabilizing polymer grafted colloids. The enthalpic mechanism can be also used to preserve the structure of block copolymer mesophases upon the addition of homopolymers.

An important property of the grafted chains is the local chain stretching. Since the location of the end point of a grafted chain depends on how much the chain is stretched, one should keep track of the end-point positions in order to study chain stretching. Because of the numerical complexity of the SCF calculations, we have integrated out this dependence. Although this does not introduce an additional approximation, it prohibits us from studying chain stretching. In the future it would be interesting to keep the end-point dependence and study in detail the local stretching of the grafted chains as well as that of the free chains.

Another simplification in this work is the assumption that the brushes are uniform in the direction parallel to the surface. For brushes in a poor solvent it was shown that the brush is unstable with respect to small "dimples" at the edge of the brush.[62] We suspect that a similar phenomenon might occur in the different dry brush regimes.

Acknowledgment. We thank D. Andelman, C. Gay, C. Ligoure, H. Orland, and Y. Tsori for valuable discussions. I.B. gratefully acknowledges the support of the French Chateaubriand postdoctoral fellowship and the hospitality of the Elf-Atochem research center at Levallois-Perret.

References and Notes

(1) De Gennes, P. G. *J. Phys. (Paris)* **1976**, *37*, 1443.
(2) De Gennes, P. G. *Macromolecules* **1980**, *13*, 1069.
(3) Alexander, S. *J. Phys. (Paris)* **1977**, *38*, 983.
(4) Semenov, A. N. *Sov. Phys. JETP* **1985**, *61*, 733.
(5) Milner, S. T.; Witten, T. A.; Cates, M. E. *Macromolecules* **1988**, *21*, 2610; **1989**, *22*, 853. For a review, see also: Milner, S. *Science* **1991**, *251*, 905.
(6) Skvortsov, A. M.; Gorbunov, A. A.; Pavlushkov, V. A.; Zhulina, E. B.; Borisov, O. V.; Priamitsyn, V. A. *Polym. Sci. USSR* **1988**, *30*, 1706. Zhulina, E. B.; Priamitsyn, V. A.; Borisov, O. V. *Polym. Sci. USSR* **1989**, *31*, 205. Zhulina, E. B.; Borisov, O. V.; Priamitsyn, V. A. *J. Colloid Interface Sci.* **1990**, *137*, 495.
(7) Brown, H. R.; Char, K.; Deline, V. R. *Macromolecules* **1989**, *23*, 3383.
(8) Witten, T.; Leibler, L.; Pincus, P. *Macromolecules* **1990**, *23*, 824.
(9) Zhulina, E. B.; Borisov, O. V.; Brombacher, L. *Macromolecules* **1991**, *24*, 4679. Zhulina, E. B.; Borisov, O. V.; Brombacher, L. *Macromolecules* **1992**, *25*, 2657.
(10) Shull, K. R. *Macromolecules* **1996**, *29*, 2659.
(11) Aubouy, M.; Raphaël, E. *J. Phys. II* **1993**, *3*, 443.
(12) Braun, H.; Rudolf, B.; Cantow, H. J. *Polym. Bull. (Berlin)* **1994**, *32*, 241.
(13) Aubouy, M.; Raphaël, E. *Macromolecules* **1994**, *27*, 5182.
(14) Leibler, L.; Ajdari, A.; Mourron, A.; Coulon, G.; Chatenay, D. In *Ordering in Macromolecular Systems;* Teramoto, A., Kobayashi, M., Norisuje, T., Eds.; Springer-Verlag: Berlin, 1994; pp 301−311.
(15) Aubouy, M.; Fredrickson, G. H.; Pincus, P.; Raphaël, E. *Macromolecules* **1995**, *28*, 2979.
(16) Martin, J. I.; Wang, Z. G. *J. Phys. Chem.* **1995**, *99*, 2833.
(17) Ligoure, C. *Macromolecules* **1996**, *29*, 5459.
(18) Gay, C. *Macromolecules* **1997**, *30*, 5939.
(19) Gast, A.; Leibler, L. *J. Phys. Chem.* **1985**, *89*, 3947; *Macromolecules* **1986**, *19*, 686.
(20) Shull, K. R. *J. Chem. Phys.* **1991**, *94*, 5723.
(21) Wijmans, C. M.; Zhulina, E. B.; Fleer, G. J. *Macromolecules* **1994**, *27*, 3238.
(22) Hasegawa, R.; Aoki, Y.; Doi, M. *Macromolecules* **1996**, *29*, 6656.
(23) Ferreira, P. G.; Ajdari, A.; Leibler, L. *Macromolecules* **1998**, *31*, 3994.
(24) Yerushalmi-Rozen, R.; Klein, J.; Fletters, L. J. *Science* **1994**, *263*, 793.
(25) Clarke, C. J.; Jones, R. A. L.; Edwards, J. L.; Shull, K. R.; Penfold, J. *Macromolecules* **1995**, *28*, 2042.
(26) Reiter, G.; Auroy, P.; Auvray, L. *Macromolecules* **1996**, *29*, 2150.
(27) Kerle, T.; Yerushalmi-Rozen, R.; Klein, J. *Macromolecules* **1998**, *31*, 422.
(28) Borukhov, I.; Leibler, L. *Phys. Rev. E* **2000**, *62*, R41.
(29) For reviews see: Binder, K. *Adv. Polym. Sci.* **1994**, *112*, 181. Matsen, M. W.; Schick, M. *Curr. Opin. Colloid Interface Sci.* **1996**, *1*, 329. Bates, F. S.; Fredrickson, G. H. *Phys. Today* **1999**, 52 (2), 32.
(30) *Macromolecules* **1992**, *25*, 4967; **1993**, *26*, 2273.
(31) Thomas, E. L. *Polym. Prepr.* **1999**, *40*, 973.
(32) Edwards, S. F. *Proc. Phys. Soc.* **1965**, *85*, 613; **1966**, *88*, 265.
(33) Doi, M.; Edwards, S. F. *The Theory of Polymer Dynamics;* Clarendon Press: Oxford, 1986.
(34) Scheutjens, J. M. H. M.; Fleer, G. J. *J. Phys. Chem.* **1979**, *83*, 1619.
(35) Fleer, G. J.; Cohen Stuart, M. A.; Scheutjens, J. M. H. M.; Cosgrove, T.; Vincent, B. *Polymers at Interfaces;* Chapman & Hall: London, 1993.
(36) Hirz, S. Unpublished thesis, University of Minnesota.

(37) Cosgrove, T.; Heath, T.; van Lent, B.; Leermakers, F.; Scheutjens, J. *Macromolecules* **1987**, *20*, 1692.
(38) Zhulina, E. B.; Borisov, O. V.; Birshtein, T. M. *J. Phys. II* **1992**, *2*, 63. Zhulina, E. B.; Borisov, O. V. *Macromolecules* **1998**, *31*, 7413.
(39) Shim, D. F. K.; Cates, M. E. *J. Phys. (Paris)* **1989**, *50*, 3535.
(40) Milner, S. T.; Wang, Z. G.; Witten, T. A. *Macromolecules* **1989**, *22*, 489.
(41) Witten, T. A.; Leibler, L.; Pincus, P. A. *Macromolecules* **1990**, *23*, 824.
(42) Likhtman, A. E.; Semenov, A. N. *Europhys. Lett.* **2000**, *51*, 307.
(43) Venema, P.; Odijk, Th. *J. Phys. Chem.* **1992**, *96*, 3922.
(44) Netz, R. R.; Schick, M. *Europhys. Lett.* **1997**, *87*, 37; *Macromolecules* **1998**, *31*, 5105.
(45) Mansfield, T. L.; Iyengar, D. R.; Beaucage, G.; McCarthy, T. J.; Stein, R. S.; Composto, R. J. *Macromolecules* **1995**, *28*, 492.
(46) Chakrabarti, A.; Toral, R. *Macromolecules* **1990**, *23*, 2016.
(47) Neelov, I. M.; Binder, K. *Macromol. Theory Simul.* **1995**, *4*, 119.
(48) De Gennes, P. G. *C. R. Acad. Sci. Paris II* **1985**, *300*, 839.
(49) Muthukumar, M.; Ho, J. S. *Macromolecules* **1989**, *22*, 965.
(50) Patel, S.; Tirrell, M.; Hadziioannou, G. *Colloids Surf.* **1988**, *31*, 157.
(51) Murat, M.; Grest, G. S. *Phys. Rev. Lett.* **1989**, *63*, 1074.
(52) Toral, R.; Chakrabarti, A.; Dickman, R. *Phys. Rev. E* **1994**, *50*, 343.
(53) Israelachvili, J. N. *Intermolecular and Surface Forces*, 2nd ed.; Academic Press: London, 1980.
(54) Sato, T.; Tsujita, Y.; Takizawa, A.; Kinoshita, T. *Macromolecules* **1991**, *24*, 158.
(55) Ziaee, S.; Paul, D. R. *J. Polym. Sci., Part B* **1996**, *34*, 2461.
(56) If the polymer melt is replaced with a diluted solution containing polymer chains as well as a small solvent, the volume fraction of polymer in the solution will provide an additional control parameter. Here we are only interested in pure polymeric systems.
(57) The distinction between short and long P chains depends also on σ and N and will be chosen below to match the crossover in the limiting behavior.
(58) Note that we have used the three-dimensional Wiener measure (as indicated by a factor 3 in the exponent). In many cases, the one-dimensional measure is used instead. This amounts to a redefinition of the Kuhn step length: $a^2 \rightarrow 3a^2$.
(59) Dolan, A. K.; Edwards, S. F. *Proc. R. Soc. London A* **1974**, *337*, 509; **1975**, *343*, 427.
(60) Ferreira, P. G.; Leibler, L. *J. Chem. Phys.* **1996**, *105*, 9362.
(61) Israelachvili, J. N. *Proc. R. Soc. London A* **1972**, *331*, 39.
(62) Yeung, C.; Balazs, A. C.; Jasnow, D. *Macromolecules* **1993**, *26*, 1914. Huang, K.; Balazs, A. C. *Macromolecules* **1993**, *26*, 4736.

MA011351G